

## Current Profile Identification on ASDEX Upgrade via Motional Stark Effect and the CLISTE Interpretive Equilibrium Code

P.J. Mc Carthy<sup>+</sup>, R.C. Wolf<sup>\*</sup>, J. Hobirk<sup>\*</sup>, H. Meister<sup>\*</sup>, W. Schneider<sup>\*</sup>

<sup>+</sup>Physics Dept., University College Cork, Association EURATOM-DCU, Cork, Ireland

<sup>\*</sup>Max-Planck-Institut für Plasmaphysik, Euratom Association, Boltzmannstrasse 2, D-85748 Garching, Germany

### 1. Introduction

The standard method for realtime plasma parameter identification and aftershot recovery of equilibrium flux surfaces from magnetic measurements on the ASDEX Upgrade tokamak is Function Parameterization (FP) [1]. Though FP can process any combination of diagnostic data, the construction of a training database of simulated equilibria with the predictive Garching Equilibrium Code (GEC) [2] uses a specific parameterization of the equilibrium pressure and poloidal current source profiles, which cannot be changed without an expensive regeneration of the database. This flexibility is desirable, however, to fully exploit current density profile information now available from the Motional Stark Effect diagnostic [3]. Accordingly, the GEC has evolved into a full interpretive equilibrium code, CLISTE [4], which solves the Grad-Shafranov equation constrained by diagnostic data using an efficient algorithm similar to that of EFIT [5].

### 2. CLISTE Interpretive Equilibrium Code

The CLISTE <sup>1</sup> (CompLete Interpretive Suite for Tokamak Equilibria) code finds a numerical solution to the Grad-Shafranov equation

$$-\left(\frac{\partial^2\psi}{\partial R^2} - \frac{1}{R}\frac{\partial\psi}{\partial R} + \frac{\partial^2\psi}{\partial Z^2}\right) = \mu_o R^2 p'(\psi) + FF'(\psi) \equiv \mu_o R j_\phi \quad (1)$$

for a given set of poloidal field coil currents and limiter structures by varying the free parameters in the parameterization of the  $p'(\psi)$  and  $FF'(\psi)$  source profiles which define the toroidal current density profile  $j_\phi$  so as to obtain a best fit in a least squares sense to a set of experimental measurements. These measurements can include external magnetic data, MSE data,  $q$ -profile information from SXR measurements, etc., and the free parameters are varied such that the penalty or *cost function*, i.e. the squared modulus of the vector of (weighted) differences between the set of experimental measurements and those predicted by the equilibrium solution, is minimized. The two source profiles in (1) are constructed by a linear superposition of basis functions, either cubic splines or polynomials, the magnitudes of which constitute the set of free parameters to be fitted. Among the features of the code are the inclusion of scrape-off layer (SOL) currents in the equilibrium calculations under the assumption that  $\mathbf{J} \times \mathbf{B} = \nabla p$  also holds in the SOL. The current density is truncated where the open field lines intersect material structures. Return currents through these structures are neglected.

At the location of each of the 10 MSE channels, the MSE diagnostic [3] provides the pitch angle-related quantity  $\tan \gamma_m$  which is related to the components of the magnetic

---

<sup>1</sup> *klis̄h-teh*, Gaelic for clever

and radial electric fields  $\mathbf{B}$  and  $\mathbf{E}_r$  by

$$\tan \gamma_m^{(f/h)} = \frac{A_1 B_R + A_2 B_\phi + A_3 B_Z + A_4 E_{rR}/v_{(f/h)beam}}{A_5 B_R + A_6 B_\phi + A_7 B_Z + A_8 E_{rR}/v_{(f/h)beam} + A_9 E_{rZ}/v_{(f/h)beam}} \quad (2)$$

where  $v_{(f/h)beam}$  refers to the velocity of the full or half energy components of the injected neutrals and  $A_{1...9}$  is a vector of viewing geometry coefficients particular to each channel. To be compatible with the linear constraints of the CLISTE algorithm, these MSE data are incorporated into the linear regression to optimize the free parameters for  $j_\phi$  at each iteration cycle in the form  $\tan \gamma_m^{(f)} D = N$  for the full energy component, where  $N/D$  refers to the rhs of (2). To account for the radial electric field contribution to  $\tan \gamma_m^{(f)}$  we use data from two independent diagnostic sources: (i) the recently available half-energy MSE data [6] and (ii) toroidal and poloidal impurity rotation velocities from charge exchange spectroscopy [7]. The importance of the  $E_r$  contribution to the reconstructed  $j_\phi$  profile is considered in [6].

### 3. Illustrative Results

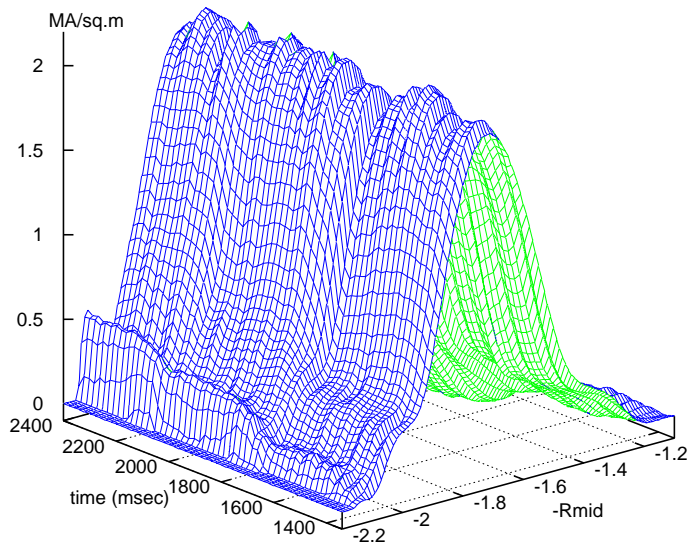


Figure 1: Time evolution of  $j_\phi$  for # 13686

corrected MSE channels spanning the range  $1.69 \leq R \leq 2.01$  or  $0 \leq \rho_{pol} \leq 0.75$ . A 12-knot parameterization was used, including knots at  $\rho_{pol} = 0.85, 0.9, 0.95, 0.98$ . The magnetics rms fit error was 0.9 mT or 1.8% of the rms signal strength while the MSE rms error was  $0.1^\circ$ . The strong edge peak in  $j_\phi$  is a robust feature of high  $\beta_{pol}$  CLISTE equilibria and is consistent with an edge peak in the bootstrap current profile which scales with  $\beta_{pol}$ . However, its identification must rely on information provided by the magnetic probes given the restricted radial range covered by the MSE channels. This conflicts with the conventional belief that diagnosis of  $j_\phi$  from external magnetics in the case of non-circular plasmas is limited to the low order moments  $I_p$ ,  $\beta_{pol}$  and  $l_i$ . Here we present evidence that identification of an edge peak in  $j_\phi$  from external magnetics is possible in the case of Xpoint plasmas.

Fig. 1 shows the time evolution of the  $j_\phi$  profile for a high  $\beta_{pol}$  lower Xpoint ASDEX Upgrade discharge # 13686,  $I_p = 400$  kA,  $B_t = -2$  T,  $3 < \bar{n}_e < 5 \times 10^{19} \text{ m}^{-3}$ , where three 2.5 MW neutral beams were switched on at  $t = 1.3$  s,  $t = 1.7$  s and  $t = 2.1$  s. The stationary values of  $\beta_{pol}$  following the activation of each NBI source are 1.3, 2.2 and 2.8, respectively. After the second source became active, the loop voltage remained close to zero. The corresponding values of the amplitude of the outboard edge peak in  $j_\phi$ , which occurs at  $\rho_{pol} \approx 0.95$ , i.e.  $\hat{\psi} \approx 0.9$ , are 0.16, 0.34 and 0.50 MA/m<sup>2</sup>. The equilibria were interpreted by CLISTE from magnetic probe data and 10  $E_r$ -

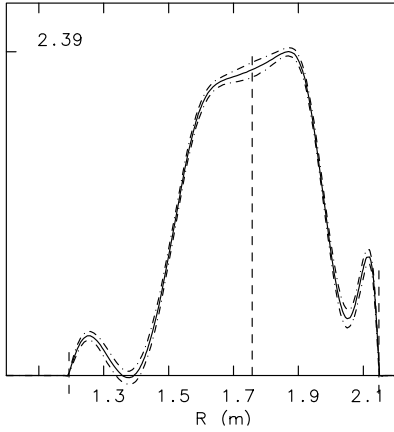


Figure 2a  $j_\phi(\text{midplane})$  for # 13685  $t=1.8\text{s}$  12-knot spline model

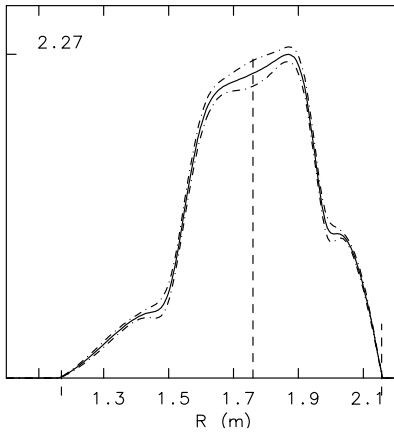


Figure 2b  $j_\phi(\text{midplane})$  for # 13685  $t=1.8\text{s}$  7-knot spline model

Fig. 2(a) shows the  $j_\phi$  profile from a CLISTE equilibrium for ASDEX Upgrade discharge # 13685,  $I_p = 800$  kA,  $B_t = -2.1$  T,  $\bar{n}_e = 5 \times 10^{19} \text{m}^{-3}$ ,  $P_{NBI} = 10$  MW,  $\beta_{pol} = 1.7$ , which has a strong edge  $j_\phi$  peak of amplitude  $0.85 \text{MA/m}^2$ . For the spline model described above, the magnetics and MSE rms fit errors were  $1.1 \text{mT}$  and  $0.16^\circ$ . Fig. 2(b) is a fit to the same timepoint, this time with no knots in the range  $0.7 < \rho_{pol} < 1.0$ . There was a modest increase to  $0.20^\circ$  in the MSE rms error, however the magnetics rms error more than doubled to  $2.5 \text{mT}$ . The separatrix strikepoint on the outboard lower divertor plate for case (a) was within 6 mm of the peak power position given by thermography. In case (b) the discrepancy was 40 mm. We investigated which probes might be responsible for identifying the edge  $j_\phi$  peak by calculating the influence of each probe signal on the  $j_\phi$  profile using the variance-covariance matrix from the final linear regression for the free parameters. If  $\mathbf{x}_i$  is the row of entries in the regression  $X$  matrix for the  $i$ th probe, i.e. the linear combination of the basis flux functions which yields the predicted value for the probe, and  $\mathbf{C}(R, Z)$  is the linear combination of the basis flux functions yielding  $j_\phi$  at location  $(R, Z)$ , then a measure of the influence of, say,  $B_{\theta_i}$  on  $j_\phi(R, Z)$ , which is related to Cook's  $D$  influence statistic [8], is given by their covariance:

$$\text{Cov}[B_{\theta_i}, j_\phi(R, Z)] = \mathbf{x}'_i \cdot \text{Vmat} \cdot \mathbf{C}(R, Z) \quad (3)$$

where  $\text{Vmat} = \sigma^2 \mathbf{X}'\mathbf{X}^{-1}$  is the variance-covariance matrix. Fig. 3 shows influence profiles for a poloidal array of 40 in-vessel tangential magnetic probes for case (a) above. Here we have plotted the squared correlation of  $B_{\theta_i}$  with  $j_\phi$  at 1% intervals along a line joining the magnetic axis to the Xpoint, with  $-1.00$  on the x-axis corresponding to the Xpoint position. There is a very prominent peak whose half maximum points occur close to probes 25 and 32 which are shown in red in Fig. 4. These probes are magnetically equidistant from the separatrix, which intersects the array close to probes 27 and 31. The probes under the correlation peak span the private flux region. The region of strong correlation extends into  $x = -0.81$  or 20 cm deep (the axis to Xpoint distance is 1.04 m). The position of the current peak itself occurs at  $x = -0.73$ , i.e. 28 cm inside the Xpoint. This distance should be contrasted with the peak-to-separatrix distance along the midplane of approx. 4 cm. Some 90 kA or 11% of the plasma current flows between the flux surface passing through the current peak and the separatrix. A CLISTE interpretation using only magnetic data yields an essentially unaltered correlation structure. When knots beyond  $\rho_{pol} = 0.7$  are excluded in this case, the magnetics error increases by 60%

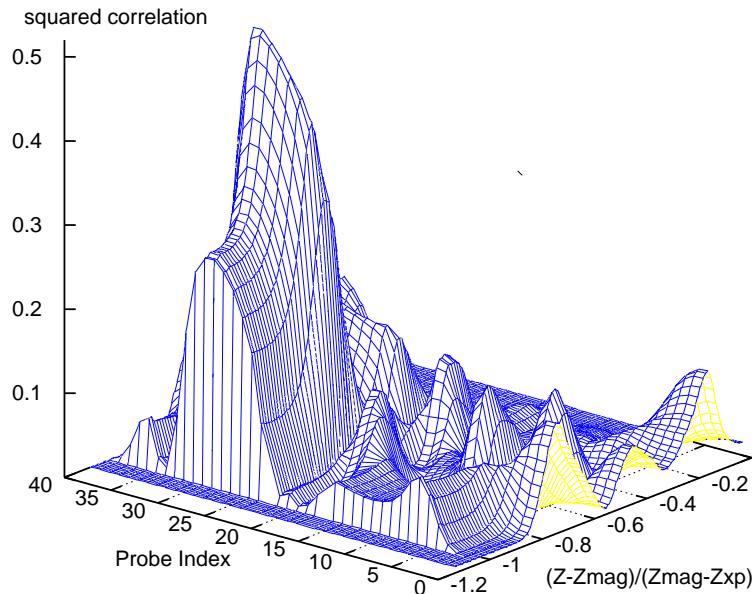


Figure 3: Influence of  $B_\theta$  Probes on Xpoint-to-magnetic axis  $j_\phi$  profile for # 13685,  $t=1.8s$

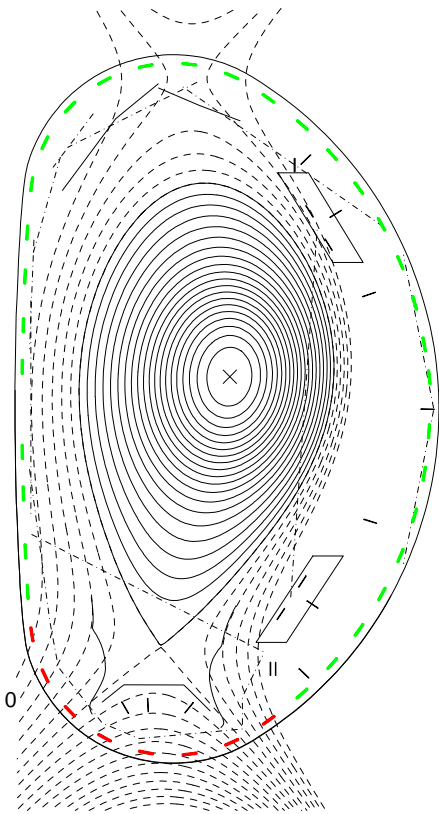


Figure 4: CLISTE equilibrium for # 13685,  $t=1.8s$ . Coloured line segments denote the 40  $B_\theta$  locations. Probes 25-32 are coloured in red

#### 4. Summary

The CLISTE code uses external magnetics and MSE data to identify current density profiles on ASDEX Upgrade [10]. The results presented here suggest that there is a hitherto unacknowledged predictive power in external magnetic probes, namely the ability to identify an edge peak in  $j_\phi$  for an Xpoint plasma. This is due to the strong correlation between the edge current peak and the probe signals spanning the private flux region, a consequence of the significant fraction of the total plasma current flowing near the Xpoint in such cases.

- [1] P.J. Mc Carthy, Ph.D. Thesis, Univ. College Cork, 1992.
- [2] K. Lackner, Comp. Phys. Commun., **12** (1976) 33.
- [3] R.C. Wolf et al., Proc. 24th Eur. Conf. on Contr. Fusion Plas. Phys. Part IV, 1509 (EPS Geneva, Berchtesgaden 1997).
- [4] P.J. Mc Carthy et al., IPP Report 5/85 (1999).
- [5] L.L. Lao et al., Nucl. Fusion **30** (1990) 1035.
- [6] J. Hobirk et al., this conference.
- [7] H. Meister et al., this conference.
- [9] R.D. Cook, Technometrics **42** (2000) 65 (reissued).
- [10] R.C. Wolf et al., Phys. Plas. **7** (2000) 1839.